

# 1 **Uncertainty Analysis in the Optimization Process of Groundwater**

## 2 **Exploitation Scheme Based on SVR Method—A Case Study of Hetao**

### 3 **Plain**

4 Yongkai An, Wenxi Lu\*, Xueman Yan

5 Corresponding author: Wenxi Lu, Email: luwenxi@jlu.edu.cn

6 Key Laboratory of Groundwater Resources and Environment, Ministry of Education, Jilin  
7 University, Changchun 130021, PR China

8 **Abstract:** This paper introduces a surrogate model to reduce the huge computational load in  
9 the process of simulation-optimization and uncertainty analysis. First, the groundwater  
10 numerical simulation model was established, calibrated and verified in the northeast of Hetao  
11 Plain. Second, two surrogate models of simulation model were established using support vector  
12 regression (SVR) method, one (surrogate model A, SMA) was used to describe the  
13 corresponding relationship between the pumping rate and average groundwater table drawdown,  
14 and another (surrogate model B, SMB) was used to express the corresponding relationship  
15 between the hydrogeological parameter values and average groundwater table drawdown. Third,  
16 an optimization model was established to search an optimal groundwater exploitation scheme  
17 using the maximum total pumping rate as objective function and the limitative average  
18 groundwater table drawdown as constraint condition, the SMA was invoked by the optimization  
19 model for obtaining the optimal groundwater exploitation scheme. Finally, the SMB was  
20 invoked in the process of uncertainty analysis for assessing the reliability of optimal  
21 groundwater exploitation scheme. Results show that the relative error and root mean square  
22 error between simulation model and the two surrogate models are both less than 5%, which is  
23 a high approximation accuracy. The SVR surrogate model developed in this study could not  
24 only considerably reduce the computational load, but also maintain high computational  
25 accuracy. The optimal total pumping rate is 7947 m<sup>3</sup>/d and the reliability of optimal scheme is  
26 40.21%. This can thus provide an effective method for identifying an optimal groundwater  
27 exploitation scheme and assessing the reliability of scheme quickly and accurately.

28 **Keywords:** surrogate model; SVR; simulation-optimization; uncertainty analysis

## 29 1. Introduction

30 Simulation-optimization approach can solve the groundwater optimization  
31 problem, by which the optimal decision-making scheme should be obtained by  
32 optimizing the decision-making input scheme under the given objectives and  
33 constraints<sup>[1-3]</sup>. Uncertainty analysis can assess the reliability of groundwater  
34 exploitation scheme due to uncertainty of hydrogeological parameter values<sup>[4-5]</sup>.  
35 However, the simulation model is invoked repeatedly in the process of simulation-  
36 optimization and uncertainty analysis, which will produce a huge computational load.  
37 Therefore, it is of great significance to reduce the computational load so as to identify  
38 an optimal groundwater exploitation scheme and assess the reliability of groundwater  
39 exploitation scheme quickly and accurately.

40 In recent years, some scholars have proposed a surrogate model of simulation  
41 model, which was used to solve optimization issue of groundwater exploitation scheme  
42 and identification of groundwater pollution sources<sup>[6-8]</sup>. The results show that it can not  
43 only reduce the computational load but also maintain high computational accuracy after  
44 introducing the surrogate model. The frequently used surrogate models include the BP  
45 neural network model, the RBF neural network model, the kriging model, the SVR  
46 model and so on<sup>[9-13]</sup>. Then the SVR model had been proved to be suitable as surrogate  
47 model because it has high computational accuracy<sup>[14-15]</sup>. Nowadays, there have been no  
48 reports on uncertainty analysis in the optimization process of groundwater exploitation  
49 scheme based on SVR model.

50 In this paper, a groundwater numerical simulation model was established,  
51 calibrated and verified in the northeast of Hetao Plain. Then SMA was established and  
52 verified using SVR method, which was used to describe the corresponding relationship  
53 between the pumping rate and average groundwater table drawdown. Afterwards, an  
54 optimization model was established to search an optimal groundwater exploitation  
55 scheme using the maximum total pumping rate as objective function and the limitative  
56 average groundwater table drawdown as constraint condition, the SMA was invoked by  
57 the optimization model for obtaining the optimal groundwater exploitation scheme.

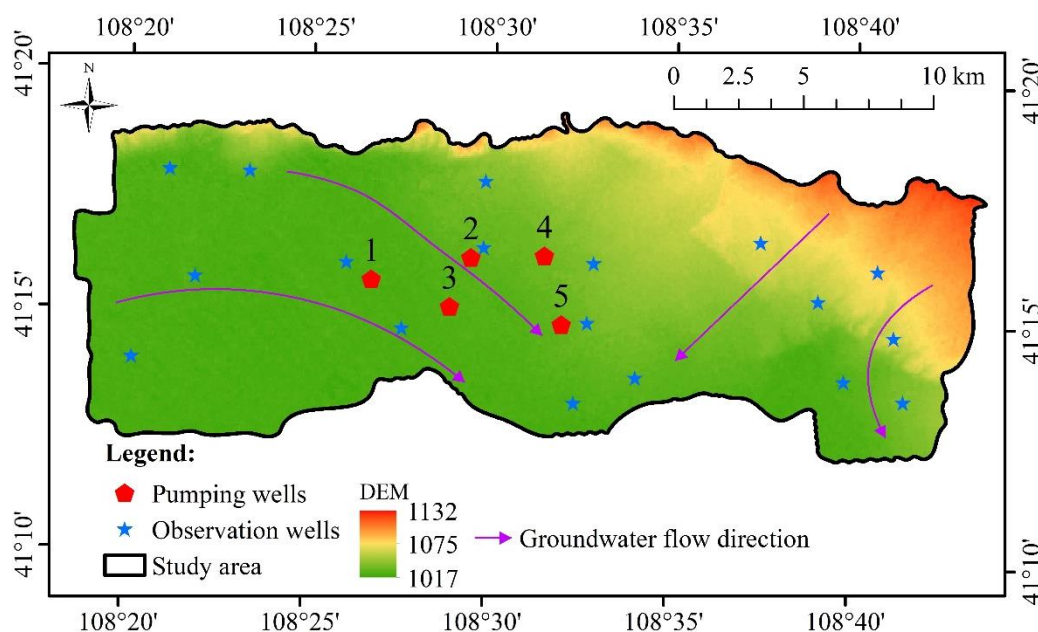
58 Finally, the SMB was established and verified using SVR method again, which was  
59 used to express the corresponding relation between the hydrogeological parameter  
60 values and average groundwater table drawdown, then the SMB was invoked in the  
61 process of uncertainty analysis for assessing the reliability of optimal groundwater  
62 exploitation scheme.

## 63 **2. Study Area and Methods**

### 64 *2.1 Study Area*

65 The study area is located in the northeastern Hetao Plain, china, where belongs to  
66 the temperate continental arid and semi-arid monsoon climate zone. The geographic  
67 coordinate lies between  $108^{\circ}18' \sim 108^{\circ}44'$  east longitude and  $41^{\circ}11' \sim 41^{\circ}21'$  north  
68 latitude. The average annual precipitation in this region is about 175 mm, and its  
69 temporal-spatial distribution is extremely uneven. The precipitation is mainly occurred  
70 in july, august and september, accounting for more than 60% of the whole year. The  
71 potential average annual evaporation is about 2084 mm, which is extremely intense.

72 There are unconfined aquifer and confined aquifer in the study area. The aimed  
73 aquifer in this study is the unconfined aquifer. The medium types of aquifer are mainly  
74 alluvial sand and gravel. The groundwater resource in the study area is very rich  
75 because of large aquifer thickness and good groundwater runoff conditions. The major  
76 groundwater recharge source is precipitation in the study area, while the groundwater  
77 is also recharged by irrigation infiltration and seasonal river infiltration in localised  
78 areas. Groundwater is discharged in the form of evaporation and runoff in the study  
79 area under natural conditions. However, in recent years, as a result of human's demand  
80 for water resource, artificial exploitation has become the major discharge in localised  
81 areas. The distribution of groundwater observation and pumping wells and groundwater  
82 flow direction are shown in Fig.1. The observation wells were used to calibrate and  
83 verify the simulation model. The pumping wells were valid only in the process of  
84 simulation-optimization.



85  
86 **Fig.1 Distribution of groundwater observation and pumping wells and groundwater flow**  
87 **direction of study area**

## 88 2.2 Methods

### 89 (1) Support vector regression

90 Support vector machine as a machine learning method, proposed by Vapnik based  
91 on VC dimension theory and structural risk minimization of statistics, is regarded as a  
92 better algorithm to substitute artificial neural network. In general, the support vector  
93 machine can solve the problems of classification and regression, replace the traditional  
94 experience risk to the minimum structure risk, and solve the actual problems which are  
95 small-scale, nonlinear and high dimensional<sup>[16-17]</sup> owing to its strict theory and  
96 mathematics foundation.

97 In this study, support vector regression (SVR) method was used to establish the  
98 surrogate model of groundwater flow numerical simulation model. The basic principle  
99 of SVR is described as follow:

100 Give  $k$  sample data,  $X = \{(x_1, y_1), (x_2, y_2), \dots, (x_k, y_k)\}$ , where  $x_i \in R^n$ , is  $n$   
101 dimensional input vector,  $y_i \in R$ , is the corresponding output variables. The basic idea  
102 is that make the dataset  $x_i$  mapped to high dimension space  $F$  where linear regression  
103 analysis is conducted simultaneously<sup>[18-19]</sup>. That is:

$$104 \quad f(x) = \omega^T \cdot \Phi(x) + b, \quad \Phi: R^n \rightarrow F, \quad \omega \in R^n \quad (1)$$

105 Where  $\omega$  is the weight value vector of hyperplane,  $b$  is the bias term.

106 Therefore, the approximation problem of regression function  $f(x)$  is equivalent  
107 to the following function:

$$108 \quad R_{reg}[f] = R_{emp}[f] + \lambda \|\omega\|^2 = \sum_{i=1}^k C(e_i) + \lambda \|\omega\|^2 \quad (2)$$

109 Where  $R_{reg}[f]$  is the objective function,  $\lambda$  is the adjustment constant,  $C(\cdot)$  is  
110 the loss function,  $\|\omega\|^2$  reflects the complexity in high dimensional space flat,  
111  $e_i = f(x_i) - y_i$ .

112 The loss function takes many forms, in view of the better sparsity of the linear loss  
113 function which is insensitive to  $\varepsilon$  [18], loss function was selected as follow:

$$114 \quad |y - f(x)|_{\varepsilon} = \max\{0, |y - f(x)| - \varepsilon\} \quad (3)$$

115 The empirical risk function was:

$$116 \quad R_{emp}^{\varepsilon}[f] = \frac{1}{k} \sum_{i=1}^k |y - f(x)|_{\varepsilon} \quad (4)$$

117 The method of obtaining loss function was equivalent to solve the following  
118 optimization problem:

$$119 \quad s.t. \begin{cases} y_i - (\omega, \Phi(x)) - b \leq \varepsilon + \xi_i^* \\ (\omega, \Phi(x)) + b - y_i \leq \varepsilon + \xi_i \\ \xi_i^*, \xi_i \geq 0 \end{cases} \quad (5)$$

120 Where  $C$  is the weighting parameter used for balancing complex term and training  
121 error term of model,  $\xi_i^*$  and  $\xi_i$  are the relaxation factor,  $\varepsilon$  is the insensitive loss  
122 function.

123 Finally, minimized Euclidean space norm, duality principle and Lagrange  
124 multiplier method were used to seek for the minimum  $\omega$  [20], then the linear regression  
125 function  $f(x)$  could be described as follow:

$$126 \quad f(x) = \sum_{i=1}^n (\alpha_i - \alpha_i^*) (x_i \cdot x) + b \quad (7)$$

127 Where  $n$  is the number of support vectors,  $\alpha_i, \alpha_i^*$  are the Lagrange multipliers.

128 For the support vector regression of nonlinear problem, the basic idea is making  
 129 data mapped to a high dimensional feature space via a nonlinear mapping, and linear  
 130 regression is conducted in this space. The specific process was realized through kernel  
 131 function  $k(x_i, x_j) = \Phi(x_i)\Phi(x_j)$  [21] and obtained the follow formula:

$$132 \quad \min. \frac{1}{2} \sum_{i,j=1}^k (\alpha_i - \alpha_i^*) (\alpha_j - \alpha_j^*) K(x_i, x_j) + \varepsilon \sum_{i=1}^k (\alpha_i + \alpha_i^*) - \sum_{i=1}^k y_i (\alpha_i - \alpha_i^*)$$

$$s.t. \sum_{i=1}^k (\alpha_i - \alpha_i^*) = 0 \quad (8)$$

$$0 \leq \alpha_i, \alpha_i^* \leq C, i = 1, 2, \dots, k$$

133 Then, find out the optimal solution of above optimization problem, regression  
 134 estimation function of nonlinear problem could be expressed as follow:

$$135 \quad f(x) = \sum (\alpha_i - \alpha_i^*) k(x_i, x) + b \quad (9)$$

136 Frequently used kernel functions mainly include:

137 (1) Polynomial kernel function

$$138 \quad K(x_i, x) = (x_i \cdot x + 1)^d, d = 1, 2, 3, \dots, n$$

139 (2) Gaussian radial basis function

$$140 \quad K(x_i, x) = \exp\left(-\frac{\|x_i - x\|^2}{2\sigma^2}\right)$$

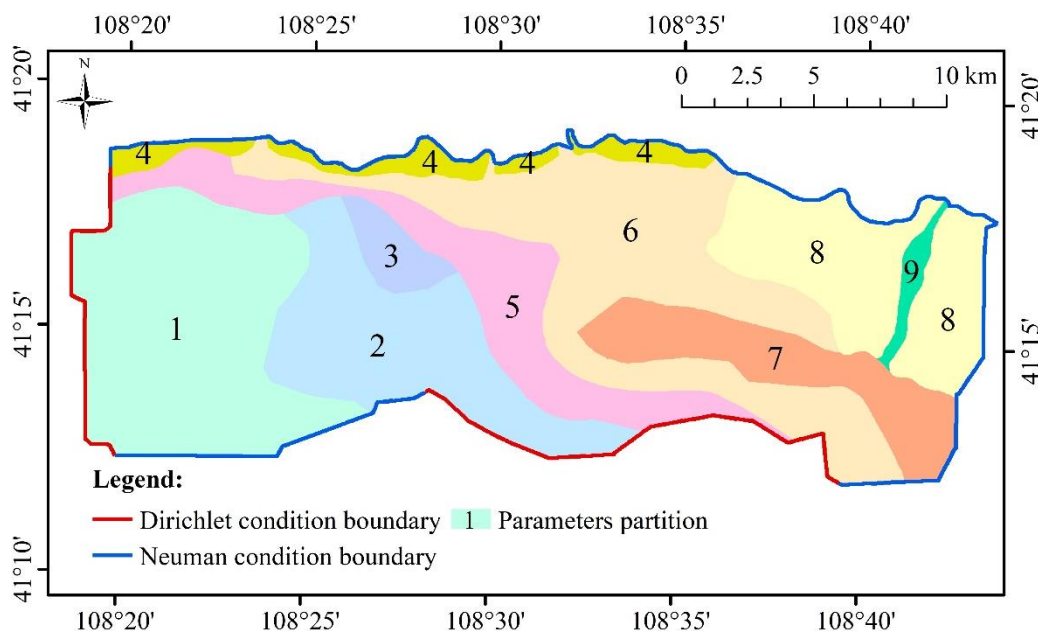
141 (3) Sigmoid kernel function

$$142 \quad K(x_i, x) = \tanh[\beta(x_i \cdot x) + c]$$

143 (2) Numerical Simulation of Groundwater Flow

144 The aimed aquifer located in the northeastern Hetao Plain is a pore aquifer. The  
 145 top of the simulation area is the unconfined aquifer's upper boundary where such  
 146 actives pertaining to water exchange mainly occur as precipitation infiltration,  
 147 irrigation leakage, evaporation, artificial exploitation, etc. The bottom of the simulation

148 area is middle pleistocene muddy silty clay which is low permeability and almost has  
149 no water exchange. The lateral boundary is generalized as shown in Fig.2.



150

151 **Fig.2 Lateral boundary types and parameter partitions of study area**

152 The groundwater flow system of the simulation area can be generalized as non-  
153 homogeneous, isotropic, and two-dimensional unsteady flow system, which can be  
154 shown as follows<sup>[22-23]</sup>:

$$\begin{aligned}
 & \frac{\partial}{\partial x} k(H(x, y, t) - Z_b) \frac{\partial H(x, y, t)}{\partial x} + \frac{\partial}{\partial y} k(H(x, y, t) - Z_b) \frac{\partial H(x, y, t)}{\partial y} \\
 & + W = \mu \frac{\partial H(x, y, t)}{\partial t} \quad (x, y) \in D, t \geq 0 \\
 & H(x, y, t) \Big|_{t=0} = H_0(x, y) \quad (x, y) \in D, t = 0 \\
 & H(x, y, t) \Big|_{\Gamma_1} = H_1(x, y, t) \quad (x, y) \in \Gamma_1, t > 0 \\
 & k(H - Z_b) \frac{\partial H}{\partial \vec{n}} \Big|_{\Gamma_2} = q(x, y, t) \quad (x, y) \in \Gamma_2, t > 0
 \end{aligned} \tag{10}$$

156 where  $H(x, y, t)$  is the groundwater table (m),  $H_0(x, y)$  is the initial water table  
157 (m),  $Z_b$  is the elevation of aimed for aquifer floor (m),  $k$  is the hydraulic  
158 conductivity ( $\text{m} \cdot \text{d}^{-1}$ ),  $\mu$  is the specific yield (dimensionless),  $W$  is the vertical  
159 recharge, discharge strength of unconfined aquifer ( $\text{m} \cdot \text{d}^{-1}$ ),  $\Gamma_1$  is the boundary of  
160 Dirichlet condition,  $\Gamma_2$  is the boundary of Neuman condition,  $q(x, y, t)$  is the

161 recharge and discharge quantity of aquifer per unit width ( $m \cdot d^{-1}$ ),  $\vec{n}$  is the direction  
162 of outward normal on the boundary,  $D$  is the area for simulation computation.

163 The parameters partitions of the study area is shown in Fig.2, in which the study  
164 area is divided into 9 subareas.

165 The Groundwater Modeling System (GMS) is made of several modular  
166 (MODFLOW, FEMWATER, MT3DMS, RT3D and so on) designed by Environmental  
167 Model Laboratory of Brigham Young University and Test Station of America Army  
168 Drainage Engineering. It was used to model groundwater flow and groundwater quality  
169 widely. MODFLOW modular of GMS (version 9.2.2) software is used to solve the  
170 numerical simulation model of groundwater, and the algorithm of MODFLOW is a  
171 finite difference method<sup>[24-26]</sup>.

### 172 (3) Monte Carlo

173 Monte Carlo simulation is also called stochastic statistical simulation. It is a  
174 computational method based on probability and statistical theory, that is, using the  
175 random numbers or pseudo-random numbers to solve the computational problem. The  
176 basic idea of Monte Carlo simulation is that the probability of the random event is  
177 estimated by the frequency of the occurrence of the random event, and as the solution  
178 of the problem which is a occurrence probability of random event<sup>[27-28]</sup>. The steps of  
179 Monte Carlo simulation are as follows<sup>[29-30]</sup>.

- 180 ① Determine random variables by means of sensitivity analysis;
- 181 ② Construct the probability distribution model of random variables;
- 182 ③ Random numbers are extracted for each input random variable;
- 183 ④ Convert the random numbers into the random samples;
- 184 ⑤ The random samples are introduced into the simulation model;
- 185 ⑥ Statistic and analysis of simulation results.

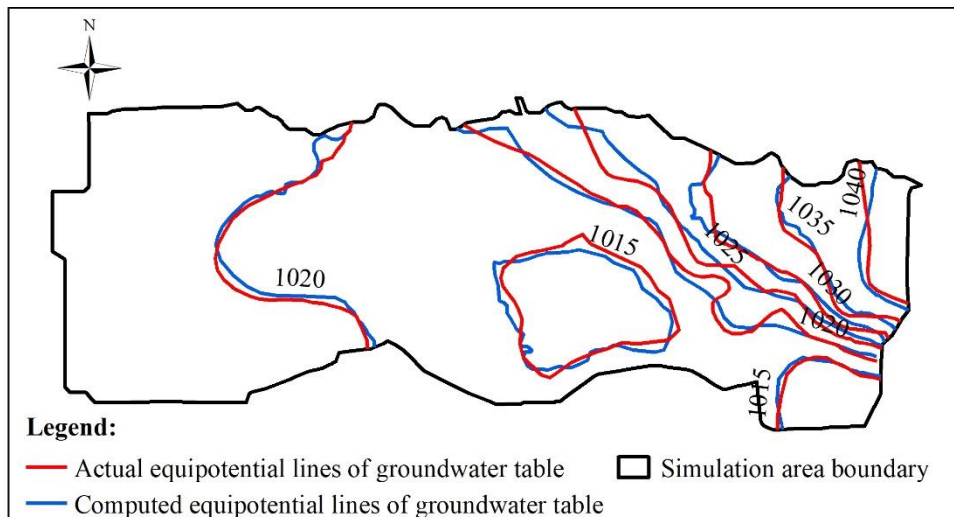
## 186 3. Results and Discussion

### 187 3.1 Numerical Simulation of Groundwater Flow

188 The calibration phase of simulation was selected in the dry season for 192 days  
189 from September 7, 2008 to March 18, 2009, taking into consideration that less source

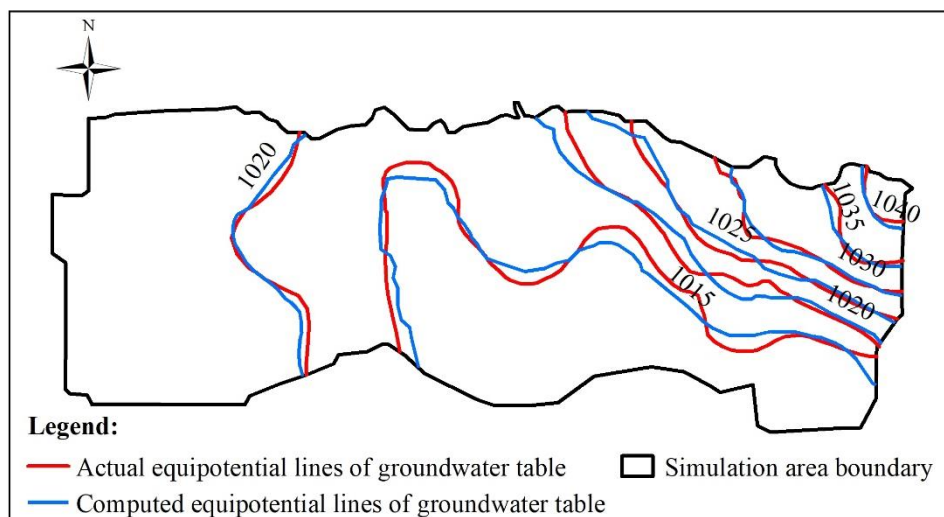


190 and sink are beneficial to identify hydrogeologic parameters. The verification phase  
 191 was selected in the wet season for 172 days from March 19, 2008 to September 7, 2008,  
 192 on account that more source and sink are beneficial to verify the effectiveness of  
 193 hydrogeologic parameters. The equipotential lines of the groundwater table are shown  
 194 in Fig.3 and Fig.4 at the end of the model calibration and verification stage respectively.



195

196 **Fig.3 The actual and computed equipotential lines of groundwater table at the end of the**  
 197 **model calibration stage**



198

199 **Fig.4 The actual and computed equipotential lines of groundwater table at the end of the**  
 200 **model verification stage**

201 From Fig.3 and Fig.4 it can be seen that the fitting results of equipotential lines  
 202 between the actual groundwater table and the computed groundwater table are very  
 203 good. The above description means that the actual measured groundwater table values

204 are very close to the computed groundwater table values, the direction of computed  
 205 groundwater flow field is in accordance with the actual groundwater flow field, the  
 206 selected hydrogeological conceptual model generalization, partial differential equations  
 207 and algorithm are reasonable and feasible, and the established numerical simulation  
 208 model of groundwater flow can objectively and accurately describe the groundwater  
 209 flow characteristics of the study area. The research results concluded above can give a  
 210 good foundation for the establishment of a surrogate model. The parameters values of  
 211 study area are shown in Table 1 after simulation model calibration and verification.

212 **Table 1 Parameters values of study subareas**

Partition	1	2	3	4	5	6	7	8	9
<b>Hydraulic conductivity</b> ( $\text{m} \cdot \text{d}^{-1}$ )	5	7.2	12.8	1.5	6.34	83	28	10	18
<b>Specific yield</b>	0.12	0.15	0.20	0.08	0.18	0.25	0.20	0.15	0.14

### 213 3.2 Optimization Model

214 In the study area, five pumping wells were set and also used as observation wells  
 215 in the process of simulation-optimization. The distribution of the five pumping wells  
 216 are shown in Fig.1. Then an optimization model was established to search an optimal  
 217 groundwater exploitation scheme using the maximum total pumping rate as objective  
 218 function and the limitative drawdown as constraint condition. The optimization model  
 219 was constructed as follows:

$$220 \quad Q = \sum_{i=1}^n q_i \quad (11)$$

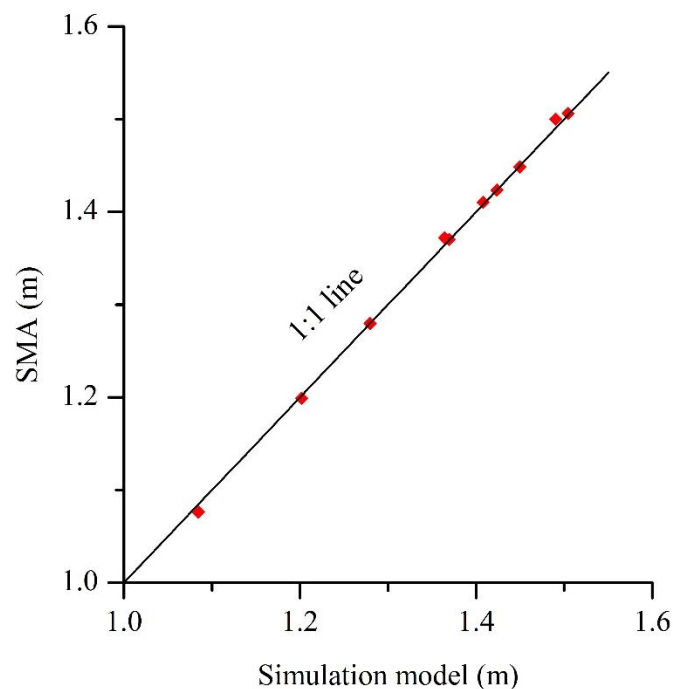
$$221 \quad \text{Subject to: } \begin{cases} \frac{1}{n} \sum_{i=1}^n s_i = \frac{1}{n} \sum_{i=1}^n f(q_i) < 1.3 \\ 0 \leq q_i \leq 2000, (i = 1, 2, 3) \\ 0 \leq q_i \leq 3000, (i = 4, 5) \end{cases} \quad (12)$$

222 where  $Q$  is the total pumping rate ( $\text{m}^3\text{d}^{-1}$ ),  $q_i$  is the pumping rate of the  $i^{\text{th}}$   
 223 well ( $\text{m}^3\text{d}^{-1}$ ),  $s_i$  is the groundwater table drawdown of the  $i^{\text{th}}$  well (m),  $n$  is the  
 224 numbers of pumping wells.

225 The optimal groundwater exploitation scheme (Maximum total pumping rate) can  
 226 be obtained by computing the optimization model. However, the simulation model is  
 227 invoked repeatedly by optimization model, which will produce a huge computational  
 228 load. Thus, a surrogate model of simulation model is introduced to reduce the huge  
 229 computational load<sup>[13,31]</sup>.

230 In order to establish the surrogate model of simulation model, the hydrogeological  
 231 parameters were considered deterministic variables, and the LHS method was used to  
 232 obtain 30 and 10 groups of exploitation schemes which were introduced into the  
 233 numerical simulation model of the groundwater flow to obtain groundwater table  
 234 drawdown datasets respectively. The former exploitation schemes were used as training  
 235 samples and the later were used as validation samples.

236 MATLAB (2017a) procedure was compiled according to the principle of the SVR  
 237 method. Training samples were used to establish the SVR surrogate model (SMA) and  
 238 validation samples were used to verify the computational accuracy of the SMA. The  
 239 fitting result and error between the simulation model and the SMA are shown in Fig.5  
 240 and Table 2, respectively.



241

242

**Fig.5 The fitting result between the simulation model and SMA**

243

**Table 2 The error between the simulation model and SMA**

Scheme	Relative Error	Mean Relative Error	Root Mean Square Error
1	0.01%	0.30%	0.55%
2	0.28%		
3	0.08%		
4	0.01%		
5	0.11%		
6	0.89%		
7	0.70%		
8	0.21%		
9	0.13%		
10	0.63%		

244 From Fig.5 and Table 2, all validation samples are close to the 1:1 line, the relative  
 245 error of each scheme is between 0.01% and 0.89%, less than 1.00%, and the mean  
 246 relative error is 0.30%, which shows that the computed groundwater table drawdown  
 247 of each scheme by the SMA is very close to the simulation model. The root mean square  
 248 error of the 10 validation schemes is 0.55%. The results show that the SMA has good  
 249 stability. The above description demonstrates that the SMA could substitute the  
 250 groundwater numerical simulation model effectively.

251 Finally, in order to solve the optimization model, the SMA was loaded into the  
 252 genetic algorithm and linked with the pumping rate. The optimal groundwater  
 253 exploitation scheme through invoking the SMA is in the Table 3.

254 **Table 3 The optimal exploitation scheme**

Pumping well	$q_1$	$q_2$	$q_3$	$q_4$	$q_5$
Pumping rate ( $\text{m}^3\text{d}^{-1}$ )	1057	725	344	2907	2914

255 From the Table 3 the max total pumping rate is  $7947 \text{ m}^3\text{d}^{-1}$ . Compared with other  
 256 wells, the pumping rate of No.2 well and No.3 well are smaller. This is due to the No.2  
 257 well and No.3 well are located at the center of the pumping wells, and long-term  
 258 exploitation is more likely to generate a large groundwater table drawdown. The results  
 259 of above quantitative and qualitative analysis show that the optimal groundwater  
 260 exploitation scheme is reasonable.

### 261 3.3 Uncertainty Analysis

262 The major influence factors that affect the simulation-optimization results include

263 the uncertainty of simulation model parameters and accuracy of surrogate model.  
 264 However, this paper only considered the uncertainty of hydrogeological parameters  
 265 (Hydraulic conductivity and specific yield) for assessing the reliability of optimal  
 266 groundwater exploitation scheme because the surrogate model has a very high accuracy.

267 In general, the monte carlo simulation method is used for uncertainty analysis.  
 268 However, the simulation model is invoked repeatedly in the process of uncertainty  
 269 analysis (Monte carlo simulation), which will produce a huge computational load. Thus,  
 270 a surrogate model of simulation model is introduced to reduce the huge computational  
 271 load<sup>[32-33]</sup>.

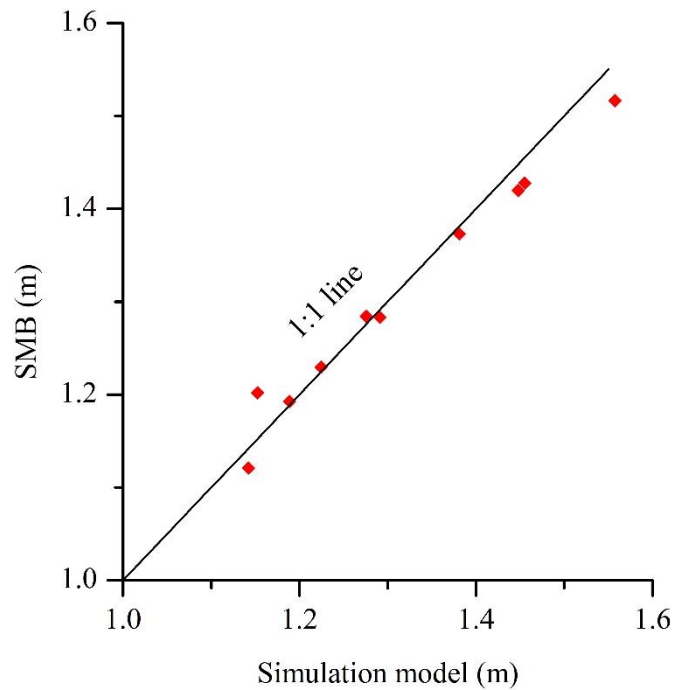
272 The reasonable regions and probability distribution types of hydrogeological  
 273 parameters had to be known before establishing the surrogate model of simulation  
 274 model. According to the actual conditions of study area and past experience, the  
 275 reasonable regions and probability distribution types of hydrogeological parameters<sup>[34]</sup>  
 276 in this study are shown in Table 4.

277 **Table 4 Reasonable regions and probability distribution types of hydrogeological**  
 278 **parameters**

Hydrogeological parameters	Reasonable region	Probability distribution type
Hydraulic conductivity	[70% of the mean,	Normal distribution
Specific yield	130% of the mean]	Uniform distribution

279 In order to establish the surrogate model of simulation model, the optimal  
 280 exploitation scheme was considered deterministic variable, and the LHS method was  
 281 used to obtain 30 and 10 groups of hydrogeological parameters which were also  
 282 introduced into the numerical simulation model of the groundwater flow to obtain  
 283 groundwater table drawdown datasets respectively. The former samples were used as  
 284 training samples and the latter were used as validation samples.

285 The training samples were used to establish the SVR surrogate model (SMB) and  
 286 validation samples were used to verify the computational accuracy of the SMB. The  
 287 fitting result and error between the simulation model and theSMB are shown in Fig.6  
 288 and Table 5, respectively.



289

290

**Table 6 The fitting result between the simulation model and SMB**

291

**Table 5 The error between the simulation model and SMB**

Scheme	Relative Error	Mean Relative Error	Root Mean Square Error
1	4.24%	2.23%	3.88%
2	3.66%		
3	0.63%		
4	0.39%		
5	2.65%		
6	1.92%		
7	4.30%		
8	1.88%		
9	0.60%		
10	1.97%		

292

From Fig.6 and Table 5, all validation samples are close to the 1:1 line, the relative error of each scheme is less than 5%, and the root mean square error of each scheme is also less than 5%. The above description demonstrates that the SMB could substitute the groundwater flow numerical simulation model effectively.

296

Finally, the LHS method was used to obtain 10000 groups of hydrogeological parameters which were also introduced into the SMB to obtain groundwater table drawdown datasets. The statistical results of the 10000 groups of groundwater table drawdown datasets are shown in Table 6.

299

300

**Table 6 Statistical results of average groundwater table drawdown datasets**

Interval of drawdown	[0, 1]	(1, 1.15]	(1.15, 1.3]	(1.3, 1.45]	(1.45, 1.6)	(1.6, +∞)
Number	13	455	3553	4811	1157	11
Probability	0.13%	4.55%	35.53%	48.11%	11.57%	0.11%

301 From the Table 6 the groundwater table drawdown in the study are mainly in the  
 302 range of 1.15-1.45, especially in the range of 1.3-1.45. The reliability of the optimal  
 303 scheme is 40.21%, which the average groundwater table drawdown is less than 1.3.  
 304 This also means the risk of the optimal scheme is 59.79%. Thus in order to enhance the  
 305 reliability of the optimal scheme, the penalty number should be added into the  
 306 constraint conditions of the optimization model. This approach is easy to implement,  
 307 and this paper does not discuss much.

#### 308 4. Conclusions

309 This paper introduces a SVR surrogate model to reduce the huge computational  
 310 load in the process of simulation-optimization and uncertainty analysis. The SVR  
 311 surrogate model developed in this study could not only considerably reduce the  
 312 computational load, but also maintain high computational accuracy. This paper provide  
 313 an effective method for identifying an optimal groundwater exploitation scheme and  
 314 assessing the reliability of scheme quickly and accurately.

315 The established numerical simulation model of groundwater flow can objectively  
 316 and accurately describe the groundwater flow characteristics of the study area. The two  
 317 SVR surrogate model both can substitute the groundwater flow numerical simulation  
 318 model for simulation and prediction. The optimal total pumping rate is 7947 m<sup>3</sup>/d and  
 319 the reliability of optimal scheme is 40.21%. In order to enhance the reliability of the  
 320 optimal scheme, the penalty number should be added into the constraint conditions of  
 321 the optimization model.

#### 322 Acknowledgments

323 This research was funded by the China Geological Survey (No. DD20160266),  
 324 China National Natural Science Foundation (41372237) and Project 2017149  
 325 Supported by Graduate innovation Fund of Jilin University.

## 326 **References**

- 327 [1] Singh A. Simulation–optimization modeling for conjunctive water use  
328 management[J]. *Agricultural Water Management*, 2014, 141(141):23-29.
- 329 [2] Zhou H B, Chen T B, Gao D, et al. Simulation of water removal process and  
330 optimization of aeration strategy in sewage sludge composting[J]. *Bioresour Technol*,  
331 2014, 171:452-460.
- 332 [3] Alizadeh H, Mousavi S J. Coupled stochastic soil moisture simulation-optimization  
333 model of deficit irrigation[J]. *Water Resources Research*, 2013, 49(7):4100–4113.
- 334 [4] Bobba A G, Singh V P, Bengtsson L. Application of uncertainty analysis to  
335 groundwater pollution modeling[J]. *Environmental Geology*, 1995, 26(2):89-96.
- 336 [5] Baalousha H M. Risk assessment and uncertainty analysis in groundwater  
337 modelling[J]. *Rwth Aachen*, 2002.
- 338 [6] Sreekanth J, Datta B. Coupled simulation-optimization model for coastal aquifer  
339 management using genetic programming-based ensemble surrogate models and  
340 multiple-realization optimization[J]. *Water Resources Research*, 2011, 47(4):158-166.
- 341 [7] Sreekanth J, Datta B. Multi-objective management of saltwater intrusion in coastal  
342 aquifers using genetic programming and modular neural network based surrogate  
343 models[J]. *Journal of Hydrology*, 2010, 393(3–4):245-256.
- 344 [8] Gu W, Lu W, Zhao Y, et al. Identification of groundwater pollution sources based  
345 on a modified plume comparison method[J]. *Water Science & Technology Water  
346 Supply*, 2017, 17(1).
- 347 [9] Sreekanth J, Datta B. Multi-objective management of saltwater intrusion in coastal  
348 aquifers using genetic programming and modular neural network based surrogate  
349 models[J]. *Journal of Hydrology*, 2010, 393(3–4):245-256.
- 350 [10] Zhou Z, Ong Y S, Nair P B, et al. Combining global and local surrogate models to  
351 accelerate evolutionary optimization[J]. *IEEE Transactions on Systems Man &  
352 Cybernetics Part C*, 2006, 37(1):66-76.
- 353 [11] Simpson T W, Mauery T M, Korte J J, et al. Kriging Models for Global  
354 Approximation in Simulation-Based Multidisciplinary Design Optimization[J]. *Aiaa*



- 355 Journal, 2001, 39(12):2233-2241.
- 356 [12] Gorissen D, Couckuyt I, Demeester P, et al. A Surrogate Modeling and Adaptive  
357 Sampling Toolbox for Computer Based Design[J]. Journal of Machine Learning  
358 Research, 2010, 11(1):2051-2055.
- 359 [13] An Y K, Lu W X, Dong H B, et al. Surrogate model of numerical simulation model  
360 of groundwater based on Kriging[J]. Zhongguo Huanjing Kexue/china Environmental  
361 Science, 2014, 34(4):1073-1079.
- 362 [14] Zhou J, Turng L S. Process optimization of injection molding using an adaptive  
363 surrogate model with Gaussian process approach[J]. Polymer Engineering & Science,  
364 2007, 47(5): 684-694.
- 365 [15] Forrester A, Keane A. Engineering design via surrogate modelling: a practical  
366 guide[M]. John Wiley & Sons, 2008.
- 367 [16] Hui D, He-Lin F U, Leng W M. Support Vector Machines For Time Series  
368 Regression and Prediction[J]. Journal of System Simulation, 2006, 18(7):1785-1788.
- 369 [17] Peng J, Li L. Support vector regression in sum space for multivariate calibration[J].  
370 Chemometrics & Intelligent Laboratory Systems, 2014, 130(2):14-19.
- 371 [18] Kavaklioglu K. Support vector regression model based predictive control of water  
372 level of U-tube steam generators[J]. Nuclear Engineering & Design, 2014, 278:651-  
373 660.
- 374 [19] Qin L T, Liu S S, Liu H L, et al. Support vector regression and least squares support  
375 vector regression for hormetic dose-response curves fitting[J]. Chemosphere, 2010,  
376 78(3):327-34.
- 377 [20] Wu J L, Yang S X, Liu C S. Parameter selection for support vectormachines based  
378 on genetic algorithms to short-term power load forecasting[J]. Journal of Central South  
379 University, 2009, 40(1):180-184.
- 380 [21] Msiza I S, Nelwamondo F V, Marwala T. Water Demand Prediction using Artificial  
381 Neural Networks and Support Vector Regression[J]. Journal of Computers, 2008, 3(11):  
382 1-8.
- 383 [22] Bear J. Dynamics of fluids in porous media[M]. Courier Corporation, 2013.
- 384 [23] Todd D K. Ground water hydrology[M]. John Wiley and Sons, Inc, New York,

385 1959.

386 [24] Du S, Su X, Zhang W. Effective storage rates analysis of groundwater reservoir  
387 with surplus local and transferred water used in Shijiazhuang City, China[J]. *Water and*  
388 *Environment Journal*, 2013, 27(2): 157-169.

389 [25] Zekri S, Triki C, Al-Maktoumi A, et al. An optimization-simulation approach for  
390 groundwater abstraction under recharge uncertainty[J]. *Water resources management*,  
391 2015, 29(10): 3681-3695.

392 [26] Spanoudaki K, Stamou A I, Nanou-Giannarou A. Development and verification of  
393 a 3-D integrated surface water-groundwater model[J]. *Journal of Hydrology*, 2009,  
394 375(3): 410-427.

395 [27] Mooney C Z. Monte carlo simulation[M]. Sage Publications, 1997.

396 [28] Binder K, Heermann D, Roelofs L, et al. Monte Carlo simulation in statistical  
397 physics[J]. *Computers in Physics*, 1993, 7(2): 156-157.

398 [29] Nylund K L, Asparouhov T, Muthén B O. Deciding on the number of classes in  
399 latent class analysis and growth mixture modeling: A Monte Carlo simulation study[J].  
400 *Structural equation modeling*, 2007, 14(4): 535-569.

401 [30] Brémaud P. Markov chains: Gibbs fields, Monte Carlo simulation, and queues[M].  
402 Springer Science & Business Media, 2013.

403 [31] Luo J, Lu W. Sobol'sensitivity analysis of NAPL-contaminated aquifer  
404 remediation process based on multiple surrogates[J]. *Computers & Geosciences*, 2014,  
405 67: 110-116.

406 [32] Hou Z, Lu W, Chen M. Surrogate-Based Sensitivity Analysis and Uncertainty  
407 Analysis for DNAPL-Contaminated Aquifer Remediation[J]. *Journal of Water*  
408 *Resources Planning and Management*, 2016, 142(11): 04016043.

409 [33] Keating E H, Doherty J, Vrugt J A, et al. Optimization and uncertainty assessment  
410 of strongly nonlinear groundwater models with high parameter dimensionality[J].  
411 *Water Resources Research*, 2010, 46(10).

412 [34] Ou Y, Lu W, Hou Z, et al. Uncertainty analysis of groundwater solute transport  
413 based on surrogate model[J]. *China Environmental Science*, 2016, 36(4): 1119-1124.